# Mineralogy of the Panulcillo skarn copper deposit, Coquimbo Region, Chile

**Asahiko Sugaki**

Kadan 4-30-503, Aoba-ku, Sendai 980-0815, Japan

**Eduardo Campos**

Departamento de Ciencias de la Tierra, Universidad de Concepción, Casilla 3-C, Concepción, Chile

**Shoji Kojima**

Departamento de Ciencias Geológicas, Universidad Católica del Norte, Av. Angamos 0610, Casilla 1280, Antofagasta, Chile
skojima@socompa.ucn.cl

## ABSTRACT

The Panulcillo skarn copper deposit developed in an Early Cretaceous (Valanginian) volcano-sedimentary sequence intruded by a Cretaceous diorite. The exoskarn zone of the deposit is composed of garnet skarn comprising grandite garnet ($Ad_{12.9-47.4}$) and phlogopite with lesser amounts of diopside ($Di_{89.6-91.6}$), clintonite, pargasitic hornblende, actinolite, pumpellyite, chlorite, quartz and calcite, exhibiting characteristic Mg-Al-rich assemblages. The principal ores consist of chalcopyrite, monoclinic pyrrhotite, sphalerite, pyrite, and magnetite with small amounts of galena, and locally secondary marcasite, hematite and covellite, generally filling interstices of the garnet skarn. Chalcopyrite shows characteristic polysynthetic twinning, normally including fine star-like crystals of sphalerite as exsolution products. Sphalerite contains 14.4 - 22.5 mol% FeS and 1.6 - 9.2 mol% MnS, and is associated intimately with chalcopyrite. It is highly likely that such Fe-rich sphalerite has coexisted primarily with hexagonal pyrrhotite under low-sulfidation conditions at higher temperatures than 275 - 254°C, below which monoclinic pyrrhotite is stable.

Key words: Cretaceous mineralization, Diorite, Grandite garnet, Magnesian skarn, Monoclinic pyrrhotite, Low sulfidation, Panulcillo copper deposit, Chile.

## RESUMEN

**Mineralogía del yacimiento cuprífero tipo skarn de Panulcillo, Región de Coquimbo, Chile**. El yacimiento tipo skarn de cobre de Panulcillo se desarrolló en una secuencia volcano-sedimentaria de edad cretácica inferior (Valanginiana), la que es intruida por un cuerpo cretácico de composición diorítica. La zona del exoskarn característicamente presenta una asociación mineralógica rica en Mg y Al, y corresponde a un skarn de granate compuesto por granate tipo ugrandita ($Ad_{12.9-47.4}$) y flogopita con candidades menores de diópsido ($Di_{89.6-91.6}$), clintonita, hornblenda pargasítica, actinolita, pumpellita, clorita, cuarzo y calcita. Los minerales metálicos consisten mayoritariamente en calcopirita, pirrotina monoclínica, esfalerita, pirita, y magnetita con menos galena, localmente marcasita, hematita y covelina secundarias, generalmente rellenando los intersticios del skarn de granate. La calcopirita exhibe maclas polisintéticas características, y normalmente contiene pequeños cristales de esfalerita en forma de estrellas como productos de exsolución. La esfalerita contiene 14,4-22,5 % molar de FeS, 1,6-9,2 % molar de MnS, y está estrechamente asociado a calcopirita. Es muy probable que este tipo de esfalerita rica en Fe originalmente haya coexistido con la pirrotina hexagonal en condiciones de baja sulfidación y temperaturas superiores a 275-254°C, dado que a temperaturas inferiores, la fase estable corresponde a pirrotina monoclínica.

Palabras claves: Mineralización cretácica, Diorita, Granate de ugrandita, Skarn magnésico, Pirrotina monoclínica, Baja sulfidación, Yacimiento cuprífero Panulcillo, Chile.

# INTRODUCTION

The Panulcillo skarn copper deposit belongs to the Lambert-Panulcillo belt located in the Coquimbo region of Chile, and is famous for producing a high grade chalcopyrite ore; the mine has produced more than 500,000 tons of ore with an average grade of 2.75 to 3.5 % Cu and 1 to 0.5 g/t Au (A. Cruzat[1]; Camus, 1986; Ardila, 1993). General descriptions of this deposit have been made by A. Cruzat (1968)[1], E.R. Carrascal[2] (1989), Ardila *et* *al.* (1991) and Ardila (1993); nevertheless, few mineralogical studies have been performed. Particularly, detailed compositional data for skarn and ore minerals have not yet been published. The objectives of this study are to describe exoskarn and ore minerals from the deposit and to specify their mineralogical and compositional character-istics, based on microscopic observations and electron microprobe analysis.
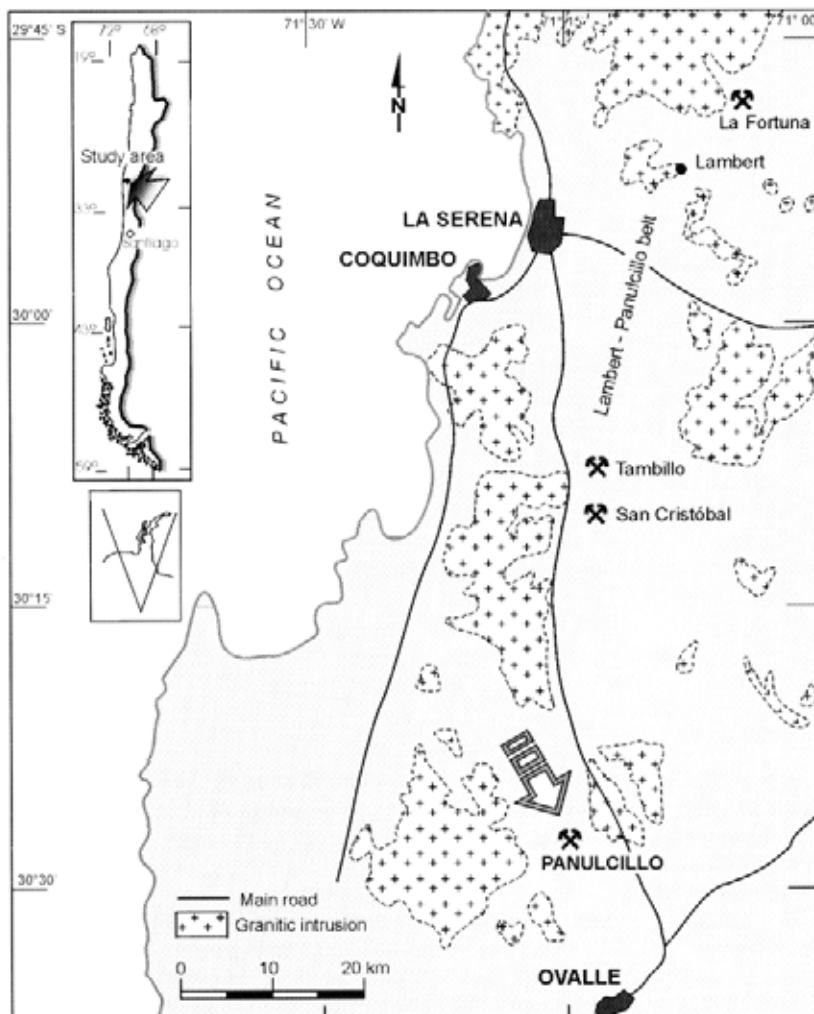


FIG. 1. Location of the Lambert-Panulcillo mining district and distribution of granitic rocks (after Moscoso *et al.*, 1982).

[1] 1968. Estudio geológico-económico del distrito minero de Panulcillo, Departamento de Ovalle, provincia de Coquimbo (Inédito), *Instituto de Investigaciones Geológicas*, 32 p.

# GENERAL GEOLOGY

The Panulcillo mine located in the Chilean Coastal Range (30°27.3'S, 71°13.1'W), about 50 km south of La Serena (Fig. 1) and 400 km north of Santiago, is a copper skarn deposit, genetically related to granitic igneous activity of Cretaceous age. The Panulcillo mining area is dominated by the Early Cretaceous (Neocomian) stratiform volcano-sedimentary formations of the Estratos de Tamaya, Estratos del Reloj and the Arqueros Formation of the Ovalle Group, in ascending order, and become younger westward in the area (Fig. 2).

The Estratos de Tamaya (Valanginian) crop out to the southeast end of the district of Panulcillo mine, and consist of andesitic lava flows and breccias intercalated with rhyolitic tuff. The Estratos del Reloj, which concordantly overlie the Estratos de Tamaya, are composed of andesitic lava flows and breccias, fosiliferous marine limestone, and red sandstones of approximately 900 m in total thickness (A. Cruzat)[1]. In general, the sequence has a N40°W trend with dips varying between 64 and 84°E (Thomas, 1967), and is separated from the Arqueros Formation by a NNW-trending fault. The Arqueros Formation is composed of porphyritic andesite ('ocoita') and sandstone of Hauterivian-Barremia age (Aguirre and Egert, 1965), and is, at least, 675 m thick (A. Cruzat)[1]. As shown in figure 2, the Panulcillo deposit resides in the lower level of the Estratos del Reloj (Valanginian stage). In the vicinity of the deposit, the sequence is intruded by a barren dioritic stock, which caused contact metamorphism and hydrothermal alteration. This obliterated the original texture of the rock and generated meta-andesite, hornfels, marble and meta-sandstone. These rocks are distributed as an elongated lens in a zone 8 km long and 500 m wide, having a north-south trend with dips of 60 to 70° east. Within the marble strata, there are three mineralized orebodies, of which the Panulcillo copper deposit is the most important (González, 1954). It is composed predominantly of garnet skarn impregnated with sulfide minerals.

Granitic rocks such as diorite, granodiorite, monzodiorite and tonalite occurring in the Coquimbo region (A. Cruzat)[1] belong to the intrusive zone of the Cretaceous magmatic arc (Moscoso et al., 1982). The granitic plutons were previously considered to have formed in Aptian-Albian time, because they intrude the Arqueros Formation (Aguirre and Egert, 1965). However, the dioritic stock located at the east of the Panulcillo mine (30°26.4'S, 71°12.5'S) has a K-Ar radiometric age of 132±7 Ma (A. Sugaki and N. Shimada)[3], indicating an older Valanginian to Hauterivian age based on the time scale by Gradstein and Ogg (1996).
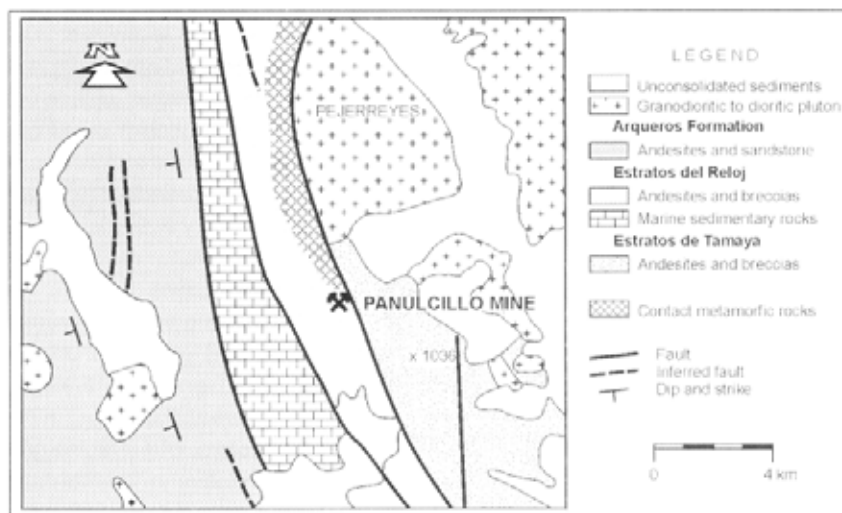


FIG. 2. Geologic map of the Panulcillo mine area (after González, 1954; Thomas, 1967).

[1] 1989. Geología del yacimiento de skarn cuprífero de Panulcillo. IV Región. Informe Interno (Inédito), Proyecto PNUD CHI88-021-ULS, 77 p.

[3] 1994. K-Ar dating on rocks and minerals related to ore deposits in Chile (2). The Science Report of Economic Geology Research Project, University of Concepción-Japan International Cooperation Agency, No. 4, p. 71-80.

## MINERALOGY AND PARAGENESIS

The Panulcillo skarn deposit is composed of an extensively developed skarn (unmineralized) zone, an ore zone and a marble zone, with the ore zone occurring as some 'baggy' forms of <160 m in length, ~40 m in width and ~50 m in height within the skarn zone (Ardila, 1993). Samples of skarn-ore and host rocks were collected from the walls of the main adit and the old stoping cave at the same level in the underground, and from the surface mine area, respectively. For approximately 40 polished sections and thin-sections of selected samples, their mineralogy and mineral paragenesis were examined by microscopic observations under both reflected and transmitted light. Chemical compositions of principal exoskarn minerals and sphalerite were determined by electron microprobe analyses mainly with JEOL JXA-8600 (GEA, Universidad de Concepción) and 8800M type (Tohoku University) instruments in conventional wavelength-dispersive methods under accelerating voltages of 15 kV and 20 kV, respectively. X-ray powder diffraction analyses by the Guinier-Hägg camera method were made for a typical garnet under operating conditions of 35-30 kV and 15-10 mA, using Cu-K $\alpha_1$ radiation monochromatized by a curved quartz crystal and metallic silicon as an internal standard. Then, crystallographic data were obtained with the method of Kitakaze (1996).

### INTRUSIVE AND HOST ROCKS

The diorite intrusive exhibits holocrystalline equigranular texture, and is mostly composed of plagioclase, biotite, hornblende, cummingtonite, clinopyroxene (augite), and orthopyroxene with small amounts of quartz, zircon, sphene, magnetite and apatite. Alkali feldspar is absent in the rock. Plagioclase, the most abundant mineral shows well-developed albite twinning and partial sericitization. Magnetite is usually fine- to medium-grained (<70 µm), including fine lamellae of exsolved ilmenite. Thus this rock shows the typical magnetite-series assemblage (Ishihara and Ulriksen, 1980; Ishihara et al., 1984).

The limestones which crop out in the mine are intruded locally by aplitic dikes, which give rise to some decimetric skarn zones (Ardila et al., 1991). The limestones are altered to crystalline marble,

containing spotty garnet and phlogopite crystals near the boundary with the exoskarn zone. Garnet is granular, partly showing optical anomaly (anomalous anisotropy) under crossed polars. Usually phlogopite occurs as layered aggregates of thick platy crystals. The marble contains disseminations of small amounts of sulfide minerals, such as pyrrhotite, chalcopyrite, pyrite, sphalerite and secondary covellite.

### SKARN AND ORE MINERALS

The exoskarn contains both a zone of calc-silicate minerals with no ore mineralization (skarn zone) and a garnet-rich zone impregnated with sulfide minerals (ore zone). It also contains phlogopite with lesser amounts of diopside, clintonite, hornblende, actinolite, pumpellyite, chlorite, quartz and calcite. A. Cruzat (1968)[1] and Ardila et al. (1991) have noted scapolite and feldspar minerals as anhydrous endoskarn in the interior of the aplitic dikes. In addition, manganese axinite has been recognized in the exoskarn zone (Ardila, 1993).

The ore minerals in the mineralized skarn include chalcopyrite, pyrrhotite, sphalerite, pyrite, and magnetite with lesser amounts of galena, secondary marcasite, hematite and covellite. Moreover, Ardila (1993) has reported the occurrence of arsenopyrite and molybdenite as minor ore minerals. Although the Panulcillo orebody contains 1 to 0.5 g/t Au as an average grade, no gold minerals, such as electrum were observed in the samples examined. The paragenetic sequence of skarn and ore minerals is shown in figure 3. As with most skarns, sulfide ore mineralization postdated the formation of anhydrous silicate minerals. Hereafter, the mode of occurrence and chemical composition of the principal minerals are described in the order: primary skarn, late stage (hydrous) skarn and ore minerals.

**Garnet:** in both skarn and ore zones, garnet is the most abundant mineral, exhibiting semitransparent dark brown, light-brown and greenish colors, euhedral to subhedral zoned grains, and locally poikiloblastic textures. In general, the garnet in the ore zone shows brownish colors, whereas the greenish garnet is observed in relatively marginal parts of the unmineralized zone near the skarn-marble contact (Ardila et al., 1991). Most garnet grains are

isotropic, but some show partly anomalous anisotropy in a zonal structure (Plate 1, Figs. a, b). Garnet grains in the marble zone and barren skarn zone appear to show the anomalous anisotropy more frequently than those in the mineralized skarn zone.

The garnet in the marble (Nos. 1-3 in Table 1) is relatively andradite-poor ($Ad_{22.8-32.4}$), whereas the garnet in the ore zone (Nos. 4-9 in Table 1) has a wider compositional range ($Ad_{12.9-47.4}$). All the garnets have trace amounts of pyrope component and variable amounts of spessartine component (2.8 - 8.7 mol% $Mn_3Al_2Si_3O_{12}$). X-ray powder diffraction data for a typical coarse-grained garnet with the intermediate composition indicate the cubic unit-cell parameter of a = 11.9235 (6) Å (Table 2). This value is compatible with the compositional data as shown in figure 4, where all electron microprobe data of the garnet are plotted in terms of the grossular-andradite pyralspite ternary diagram. Compositional variation within a typically zoned garnet (Fig. 5) was examined so as to check the relationship between the anomalous anisotropy and chemical composition. The analytical results (Table 3) show that the central part of the zoned garnet, which exhibits the anomalous anistropy (Nos. 1-6), is in the narrow range of fairly andradite-poor compositions (ca. $Ad_{24-34}$). The compositional range is similar to that of garnet in the marble zone. A similar phenomenon

has been observed in anisotropic grandite garnets from Japanese skarn deposits, which show a much wider compositional range (Mariko and Nagai, 1980).

It is evident that the greenish garnet is much more andraditic ($<Ad_{99}$; Meinert, oral communication, 2000), although such data are not provided in this study. Consequently, a wider compositional range of $Ad_{13-99}$, which is typical of most copper skarn deposits, is given for the Panulcillo garnets (Meinert, oral communication, 2000).

**Diopside:** as compared with garnet, pyroxene is scarce. However, appreciable amounts of clino-pyroxene are observed as a relict of the skarn zone exhibiting corroded forms, and are closely associated with garnet and actinolite. The compositional data (Nos. 10-12 in Table 1) show clearly that the clino-pyroxene corresponds to diopside near the Mg-end composition ($Di_{89.6-91.6}$). However, Ardila (1993) has noted less diopsidic pyroxenes ($Di_{52-82}$), which are typical of metasomatic copper skarn deposits (Meinert, 1992).

**Phlogopite:** in both skarn and marble zones, phlogopite occurs as layered aggregates of wide platy crystals with dark-green colors. In general, phlogopite shows straight extinction under crossed polars, and the skarn phlogopite is closely associated with garnet, clintonite and secondary chlorite. Electron microprobe analysis shows that the phlogopite contains appreciable amounts of Fe (2.4 – 9.0 wt%) and Mn (0.5 – 0.6 wt%) in addition to K, Mg, Al and Si (Nos. 1-4 in Table 4).

For the well-crystallized phlogopite a K-Ar radiometric age of 115 ±3 Ma has been obtained (Ardila, 1993).

**Clintonite:** in some phlogopite-rich samples, clintonite occurs as prismatic crystal aggregates, which are closely associated with garnet and phlogopite (Plate 1, Fig. c). The clintonite is nearly colorless in plane-polarized light, showing straight extinction under crossed polars. The margin of the clintonite, as well as the phlogopite, is partially changed into chlorite as a late alteration mineral. The analytical data (Nos. 5-7 in Table 4) show that the clintonite is Mg-rich, containing small amounts of Fe.

**Hornblende:** in the skarn zone, small amounts of hornblende occur as composite crystal aggregates, varying in grain size. These hornblende crystals exhibit a distinct pleochroism in dark-green colors under plane-polarized light. The hornblende usually fills the pore space between coarse-grained garnet
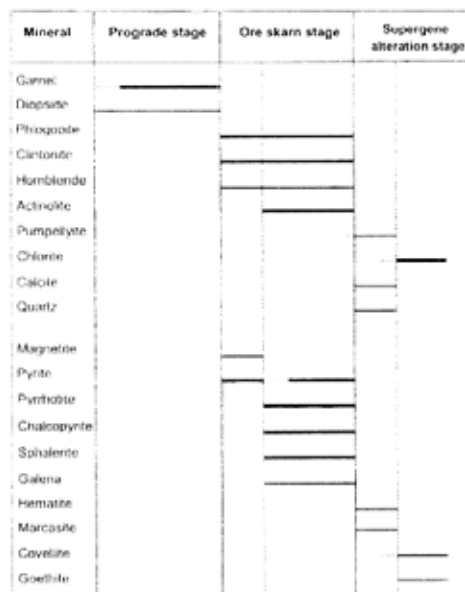


FIG. 3. Paragenetic sequence of exoskarn and ore minerals from the Panulcillo mine.

**TABLE 1. ELECTRON MICROPROBE ANALYSES OF PRIMARY SKARN MINERALS.**

| | 1 | 2 | 3 | 4 | 5 | 6 | 7 | 8 | 9 | 10 | 11 | 12 |
|---|---|---|---|---|---|---|---|---|---|---|---|---|
| **Weight percent** | | | | | | | | | | | | |
| $SiO_2$ | 38.8 | 39.2 | 38.1 | 39.0 | 37.7 | 38.5 | 37.9 | 38.2 | 37.6 | 54.3 | 55.0 | 53.2 |
| $TiO_2$ | 0.0 | 0.0 | 0.0 | 0.1 | 0.8 | 0.0 | 0.9 | 0.0 | 0.0 | 0.0 | 0.0 | 0.2 |
| $Al_2O_3$ | 16.7 | 16.6 | 14.7 | 19.1 | 16.7 | 14.8 | 12.4 | 12.2 | 11.2 | 0.5 | 0.4 | 1.3 |
| $Fe_2O_3$ | 8.4 | 7.9 | 11.0 | 4.5 | 7.8 | 10.6 | 13.0 | 14.4 | 16.0 | - | - | - |
| FeO | 0.0 | 0.6 | 0.0 | 0.7 | 0.3 | 0.7 | 0.0 | 0.0 | 0.0 | 1.5 | 1.4 | 2.0 |
| MnO | 2.6 | 2.6 | 2.4 | 4.6 | 4.1 | 2.5 | 2.1 | 1.9 | 1.6 | 1.2 | 1.3 | 1.3 |
| MgO | 0.2 | 0.2 | 0.3 | 0.2 | 0.2 | 0.1 | 0.1 | 0.1 | 0.3 | 16.7 | 16.7 | 15.9 |
| CaO | 34.1 | 33.6 | 33.5 | 31.8 | 32.1 | 33.7 | 33.5 | 33.9 | 33.8 | 26.0 | 26.0 | 25.7 |
| $Na_2O$ | 0.0 | 0.0 | 0.0 | 0.0 | 0.0 | 0.0 | 0.0 | 0.0 | 0.0 | 0.0 | 0.0 | 0.1 |
| $K_2O$ | 0.0 | 0.0 | 0.0 | 0.0 | 0.0 | 0.0 | 0.0 | 0.0 | 0.0 | 0.0 | 0.0 | 0.0 |
| | | | | | | | | | | | | |
| Total | 100.8 | 100.9 | 100.0 | 100.0 | 99.6 | 100.9 | 99.8 | 100.9 | 100.4 | 100.2 | 100.9 | 99.7 |
| | O=12 | | | | | | | | | O=6 | | |
| **Cation ratio** | | | | | | | | | | | | |
| Si | 3.00 | 3.00 | 2.99 | 3.00 | 2.95 | 3.00 | 3.00 | 3.00 | 2.99 | 1.98 | 1.99 | 1.95 |
| Ti | 0.00 | 0.00 | 0.0 | 0.01 | 0.05 | 0.00 | 0.05 | 0.00 | 0.00 | 0.00 | 0.00 | 0.01 |
| Al | 1.52 | 1.50 | 1.36 | 1.74 | 1.54 | 1.35 | 1.16 | 1.13 | 1.05 | 0.02 | 0.02 | 0.06 |
| | | | | | | | | | | | | |
| Fe(III) | 0.49 | 0.46 | 0.65 | 0.26 | 0.46 | 0.62 | 0.77 | 0.85 | 0.95 | - | - | 11 |
| Fe(II) | 0.00 | 0.04 | 0.00 | 0.05 | 0.02 | 0.05 | 0.00 | 0.00 | 0.00 | 0.04 | 0.04 | 0.06 |
| Mn | 0.17 | 0.19 | 0.16 | 0.30 | 0.27 | 0.17 | 0.14 | 0.13 | 0.11 | 0.04 | 0.04 | 0.04 |
| Mg | 0.02 | 0.02 | 0.03 | 0.02 | 0.01 | 0.02 | 0.02 | 0.04 | 0.04 | 0.91 | 0.90 | 0.87 |
| Ca | 2.81 | 2.78 | 2.81 | 2.62 | 2.70 | 2.80 | 2.85 | 2.86 | 2.87 | 1.01 | 1.01 | 1.01 |
| Na | 0.00 | 0.00 | 0.00 | 0.00 | 0.00 | 0.00 | 0.00 | 0.00 | 0.00 | 0.00 | 0.00 | 0.01 |
| K | 0.00 | 0.00 | 0.00 | 0.00 | 0.00 | 0.00 | 0.00 | 0.00 | 0.00 | 0.00 | 0.00 | 0.00 |
| Total | 8.01 | 7.99 | 8.00 | 7.99 | 8.00 | 8.00 | 7.98 | 8.00 | 8.01 | 4.01 | 4.00 | 3.99 |
| | | | | | | | | | | | | |
| **End member mol percent** | | | | | | | | | | | | |
| Pyr | 0.7 | 0.7 | 1.2 | 0.6 | 0.3 | 0.5 | 0.3 | 1.2 | 1.2 | | | |
| Alm | 0.0 | 1.2 | 0.0 | 1.4 | 0.5 | 1.5 | 0.0 | 0.0 | 0.0 | | | |
| Sps | 5.7 | 6.1 | 5.3 | 8.7 | 7.0 | 5.5 | 2.8 | 4.1 | 3.6 | | | |
| Grs | 69.4 | 69.2 | 61.1 | 76.4 | 68.7 | 61.7 | 56.8 | 52.5 | 47.8 | | | |
| And | 24.2 | 22.8 | 32.4 | 12.9 | 23.6 | 30.8 | 40.1 | 42.2 | 47.4 | | | |

1-3, garnet in limestone; 4-9, garnet in skarn-ore zone; 10-12, diopside. Abbreviations: Pyr, pyrope; Alm, almandine; Sps, spessartine; Grs, grossular. And, andradite.

**TABLE 2. X-RAY POWDER DIFFRACTION DATA FOR SKARN GARNET.**

| I/i | h | k | l | d (obs) | d (calc) |
|---|---|---|---|---|---|
| 37 | 4 | 0 | 0 | 2.982 | 2.981 |
| 100 | 4 | 2 | 0 | 2.667 | 2.666 |
| 17 | 3 | 3 | 2 | 2.544 | 2.542 |
| 37 | 4 | 2 | 2 | 2.435 | 2.434 |
| 25 | 4 | 3 | 1 | 2.340 | 2.338 |
| 16 | 5 | 2 | 1 | 2.178 | 2.177 |
| 22 | 5 | 3 | 2 | 1.9348 | 1.9343 |
| | 6 | 1 | 1 | - | 1.9343 |
| 8 | 6 | 2 | 0 | 1.8867 | 1.8853 |
| 12 | 4 | 4 | 4 | 1.7204 | 1.7210 |
| 18 | 6 | 4 | 0 | 1.6535 | 1.6535 |
| 3 | 6 | 3 | 3 | 1.6223 | 1.6226 |
| | 5 | 5 | 2 | - | 1.6226 |
| | 7 | 2 | 1 | - | 1.6226 |
| 48 | 6 | 4 | 2 | 1.5935 | 1.5934 |
| 7 | 8 | 0 | 0 | 1.4896 | 1.4904 |
| 2 | 7 | 4 | 3 | 1.3858 | 1.3861 |
| | 8 | 3 | 1 | - | 1.3861 |
| 10 | 8 | 4 | 0 | 1.3334 | 1.3331 |
| 15 | 8 | 4 | 2 | 1.3012 | 1.3010 |
| 5 | 8 | 6 | 4 | 1.1071 | 1.1071 |
| | 10 | 4 | 0 | - | 1.1071 |

Cell parameter: a = 11.9235 (6) Å.

crystals in the unmineralized zone, but has not been observed in the ore zone. The hornblende is relatively rich in Al, Na and K and poor in Si (5.82-5.91 in formula), with a Mg/Mg+Fe ratio from 0.756 to 0.784 (Nos. 8-10 in Table 4). According to the classification of Leake (1978) and IMA (1997), such a hornblende corresponds to pargasite or ferropargasite.

**Actinolite**: small amounts of actinolite are observed in the skarn and ore zones, showing radial fibrous aggregates. Actinolite usually occurs interstitially to garnet crystals and in small veinlets cutting the garnet skarn zone (Plate 1, Fig. d). The former is frequently replaced by chlorite as the late alteration mineral. In the veinlets, actinolite is closely associated with sulfide minerals, such as pyrite, chalcopyrite and sphalerite. The analytical data (Nos. 11-12 in Table 4) indicate that the actinolite is moderately Si- and Fe-rich (Mg/Mg+Fe=0.42-0.44), corresponding to ferroactinolite according to the classification of IMA (1997).

**Pumpellyite**: a trace amount of pumpellyite has been observed in pore space of the skarn zone, occurring as tiny polyhedral crystals. This mineral exhibits the characteristic interference colors of yellow to deep blue, being similar to epidote in crossed-polarized light. The compositional data (Nos. 13-15 in Table 4) show that the mineral is Al-rich pumpellyite with limited Fe contents of 10 to 12 wt.%.

**Chlorite**: in the later stage of alteration, chlorite occurs as low-crystalline fibrous aggregate, locally replacing the periphery of phlogopite, clintonite and actinolite. The compositional data (Nos. 16-17 in Table 4) show that the chlorite is rich in Al (Al = 1.41-1.43 in 4 (Si, Al)), having relatively low (Fe+Mn)/(Fe+Mn) + Mg values (0.27-0.28). According to the classification of Hey (1954) and Deer et al. (1962), this type of chlorite corresponds to sheridanite - ripidolite.

**Quartz and calcite**: appreciable amounts of quartz occur as fine-grained inclusions (<20 μm) in garnet crystals or as a matrix constituent, exhibiting irregularly anhedral shapes. Calcite occurs as infillings of principal skarn minerals. These are considered to be late stage minerals.

**Chalcopyrite**: as the most abundant ore mineral, chalcopyrite occurs in the ore zone, filling interstices of the garnet skarn (Plate 1, Fig. e). Chalcopyrite commonly forms patchwork-like aggregates, frequently exhibiting polysynthetic twinning. In general, chalcopyrite is closely associated with pyrrhotite and sphalerite, having irregular interfaces with them (Plate 1, Fig. f). Frequently, chalcopyrite includes fine-grained skeletal (star-like) crystals of sphalerite (Plate 1, Fig. g), which are oriented along the twin boundary of chalcopyrite in some cases. As described below, chalcopyrite also occurs as fine bleblike crystals in sphalerite.

**Pyrrhotite**: irregular massive pyrrhotite is usually observed in close association with chalcopyrite, sphalerite and pyrite. This pyrrhotite is ferromagnetic, corresponding to the monoclinic type (4C-type; Kissin and Scott, 1982). This was substantiated by X-ray powder diffraction analysis and electron microprobe analysis. The latter shows that the pyrrhotite contains 46.6 to 47.0 at.% Fe near the ideal composition of $Fe_7S_8$ and that contents of Cu, Zn, Mn and Cd are negligible.

**Sphalerite**: in the ore zone, sphalerite also occurs as a principal mineral, and exhibits reddish-brown colors in plane-polarized transmitted light. Sphalerite frequently includes bleblike and lamellar crystals of chalcopyrite, which are oriented along certain crystallographic directions of sphalerite (Plate 1, Fig. h). Chemical compositions of sphalerite associated with pyrite and/or pyrrhotite are given in table 5. The sphalerite shows fairly Fe-rich compositions with a fairly wide FeS variation (14.4-22.5 mol% FeS), which has no major relationships with the associated Fe-sulfide minerals (Fig. 6). Furthermore, the sphalerite contains significant amounts of MnS ranging from 1.6 to 9.2 mol%. In contrast, Cu and Cd normally contained as minor elements in natural sphalerite are uniformly low.
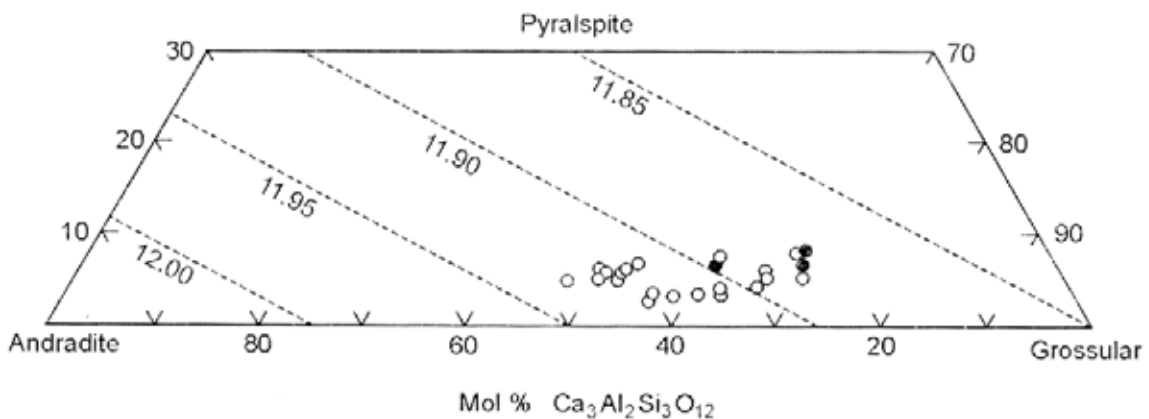


FIG. 4. Ternary plot showing relationship of composition and cell parameter of garnet from the Panulcillo mine. Solid and open circles stand for garnet in the marble zone and that in the ore zone, respectively. Data of unit-cell parameters (in Å) for garnet group minerals are represented by dotted lines (Sriramadas, 1957). See text for detailed explanations.

**Pyrite**: commonly pyrite occurs as idiomorphic to anhedral crystals, coexisting intimately with chalcopyrite, pyrrhotite and sphalerite. Microscopic observations under reflected light suggest that the pyrite is present as coarse-grained holey crystals and as irregularly-shaped grains. The former type pyrite is regarded as an earlier stage product, because the crystal is partially replaced by pyrrhotite and is overgrown with the latter type of pyrite. In a pyrite-dominant ore sample, pyrite contains minute inclusions of the chalcopyrite-pyrrhotite association.

**Magnetite**: frequently, magnetite occurs as discrete grains in the garnet skarn, being closely associated with the Cu-Fe sulfide minerals.

**Other ore minerals**: small amounts of galena are present locally in some garnet-rich samples. Hematite occurs as tiny spherulitic crystals intergrown with the principal ore minerals. Marcasite is
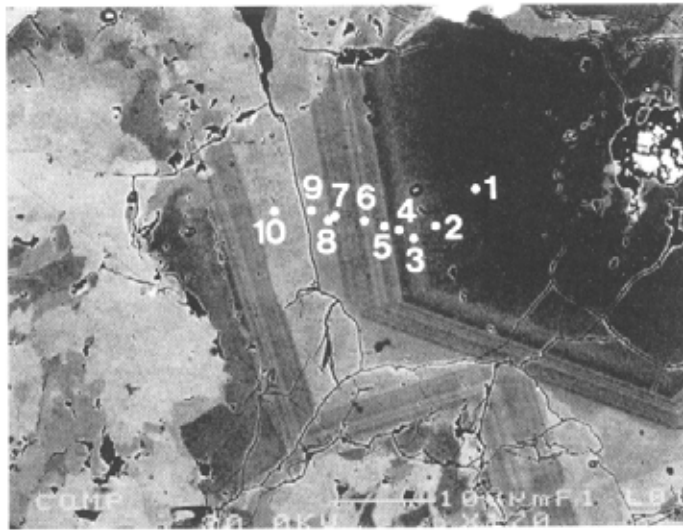


FIG. 5. Back-scattered electron image of zoned grandite garnet. Numbers 1 to 10 correspond to the analytical points of table 3.
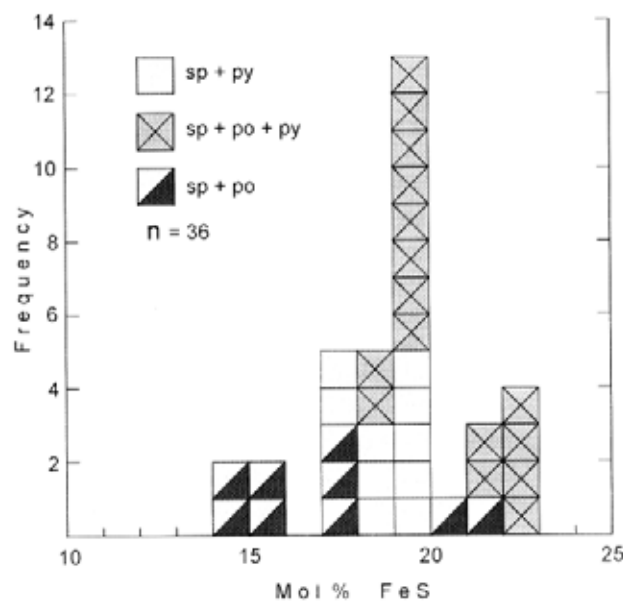


FIG. 6. Histogram of mol % FeS in sphalerite associated with pyrite and/or pyrrhotite.

TABLE 3. COMPOSITIONAL VARIATION OF ZONED GARNET OBSERVED IN FIGURE 5.

| | Central core | | | | | | | | Periphery | |
|---|---|---|---|---|---|---|---|---|---|---|
| | 1 | 2 | 3 | 4 | 5 | 6 | 7 | 8 | 9 | 10 |
| **Weight percent** | | | | | | | | | | |
| $SiO_2$ | 38.6 | 38.5 | 38.5 | 38.4 | 38.8 | 38.5 | 37.9 | 38.0 | 38.9 | 38.2 |
| $TiO_2$ | 0.2 | 0.0 | 0.1 | 0.3 | 0.2 | 0.4 | 0.3 | 0.6 | 0.3 | 0.3 |
| $Al_2O_3$ | 15.9 | 15.4 | 13.9 | 15.4 | 14.4 | 13.1 | 13.9 | 14.4 | 12.7 | 12.8 |
| $Fe_2O_3$ | 8.0 | 10.0 | 11.1 | 9.6 | 11.2 | 12.5 | 11.1 | 10.8 | 13.3 | 13.4 |
| $FeO$ | 0.0 | 0.4 | 0.0 | 0.0 | 0.0 | 0.0 | 0.0 | 0.0 | 0.0 | 0.0 |
| MnO | 2.9 | 2.4 | 2.3 | 2.5 | 2.3 | 2.1 | 2.1 | 2.1 | 1.7 | 1.8 |
| MgO | 0.1 | 0.0 | 0.1 | 0.1 | 0.1 | 0.1 | 0.2 | 0.3 | 0.3 | 0.2 |
| CaO | 34.1 | 33.7 | 34.2 | 34.1 | 33.9 | 33.6 | 34.2 | 33.8 | 33.8 | 34.0 |
| Total | 99.9 | 100.5 | 100.2 | 100.4 | 100.8 | 100.3 | 99.7 | 99.9 | 101.0 | 100.7 |
| **Cation ratio** ($O = 12$) | | | | | | | | | | |
| Si | 3.01 | 3.00 | 3.02 | 2.99 | 3.02 | 3.03 | 2.99 | 2.98 | 3.03 | 3.00 |
| Ti | 0.01 | 0.00 | 0.01 | 0.02 | 0.01 | 0.02 | 0.02 | 0.04 | 0.02 | 0.02 |
| Al | 1.46 | 1.42 | 1.29 | 1.41 | 1.32 | 1.21 | 1.29 | 1.33 | 1.17 | 1.18 |
| Fe (III) | 0.47 | 0.58 | 0.65 | 0.57 | 0.65 | 0.74 | 0.66 | 0.64 | 0.78 | 0.79 |
| Fe (II) | 0.00 | 0.02 | 0.00 | 0.00 | 0.00 | 0.00 | 0.00 | 0.00 | 0.00 | 0.00 |
| Mn | 0.19 | 0.16 | 0.16 | 0.17 | 0.15 | 0.14 | 0.14 | 0.14 | 0.11 | 0.12 |
| Mg | 0.01 | 0.00 | 0.01 | 0.01 | 0.01 | 0.01 | 0.02 | 0.03 | 0.03 | 0.03 |
| Ca | 2.90 | 2.81 | 2.87 | 2.84 | 2.83 | 2.83 | 2.90 | 2.84 | 2.83 | 2.86 |
| Total | 8.01 | 8.00 | 8.00 | 8.01 | 7.99 | 7.98 | 8.02 | 8.00 | 7.97 | 8.00 |
| **End member mol percentage** | | | | | | | | | | |
| Pyr | 0.2 | 0.1 | 0.1 | 0.3 | 0.2 | 0.3 | 0.4 | 0.7 | 0.6 | 0.5 |
| Alm | 0.0 | 0.5 | 0.0 | 0.0 | 0.0 | 0.0 | 0.0 | 0.0 | 0.0 | 0.0 |
| Sps | 4.8 | 3.8 | 3.4 | 4.0 | 3.3 | 2.9 | 3.1 | 3.1 | 2.3 | 2.4 |
| Grs | 70.5 | 66.4 | 62.8 | 66.9 | 63.3 | 59.0 | 62.6 | 63.5 | 56.9 | 56.9 |
| And | 24.4 | 29.2 | 33.7 | 28.8 | 33.1 | 37.8 | 34.0 | 32.8 | 40.2 | 40.2 |

locally associated with pyrite as irregularly-formed discrete grains or fine-grained aggregates. Covellite occurs locally as the altered product of chalcopyrite. The latter two minerals are considered to be super-gene products. Limonite (goethite) appears in the later secondary alteration stage, occurring as colloform aggregate in the pore space of garnet skarn.

## DISCUSSION

### PRIMARY SKARN FORMATION

It is significant to compare the paragenesis and chemical compositions of skarn minerals from the world's copper skarn deposits including the Lambert-Panulcillo belt, in considering the characteristics of the mineralization at the Panulcillo deposit. Several skarn copper districts and deposits are known in the belt: e.g., San Antonio, San Cristóbal (El Peñón), and Tambillo (Fig. 1). The paragenetic sequences observed in the other deposits are fairly similar to that of the Panulcillo deposit (Camus, 1986). In the Panulcillo copper skarn deposit, grandite garnet is the most abundant constituent of the exoskarn, where the pyroxene-rich skarn is poorly developed. The scarcity of pyroxene skarn is commonly observed also at the other skarn copper deposits in the Lambert-Panulcillo belt. On the other hand, such Mg-rich skarn minerals as phlogopite and clintonite, which are not observed in the other deposits, occur in the Panulcillo deposit. These minerals are rare in the majority of copper skarn deposits in the world, and so the Panulcillo exoskarns show a general feature of magnesian skarns. This may be diagnostic of a magnesian component in the original carbonate rocks.

Among the other deposits in the Lambert-Panulcillo belt, chemical data have been given only for principal skarn minerals (garnet, diopside, epidote and actinolite) from the La Fortuna deposit in the San Antonio district (M. Fukuoka et al.[3]; Ardila, 1993). The compositions of the garnet in the ore

TABLE 4. ELECTRON MICROPROBE ANALYSES OF HYDROUS SKARN MINERALS.

| | Phlogopite | | | | Clintonite | | | Hornblende | | | Actinolite | | Pumpellyite | | | Chlorite | |
|---|---|---|---|---|---|---|---|---|---|---|---|---|---|---|---|---|---|
| | 1 | 2 | 3 | 4 | 5 | 6 | 7 | 8 | 9 | 10 | 11 | 12 | 13 | 14 | 15 | 16 | 17 |
| **Weight percent** | | | | | | | | | | | | | | | | | |
| $SiO_2$ | 38.6 | 38.8 | 37.7 | 37.0 | 17.6 | 18.2 | 18.6 | 40.7 | 40.3 | 40.2 | 50.2 | 51.5 | 36.4 | 36.7 | 37.3 | 26.3 | 25.6 |
| $TiO_2$ | 0.0 | 0.1 | 0.1 | 0.2 | 0.0 | 0.0 | 0.0 | 0.1 | 0.2 | 0.2 | 0.0 | 0.0 | 0.2 | 0.3 | 0.0 | 0.0 | 0.0 |
| $Al_2O_3$ | 19.0 | 19.0 | 18.9 | 17.8 | 41.3 | 40.2 | 40.4 | 16.7 | 17.4 | 17.6 | 2.2 | 2.1 | 21.8 | 22.1 | 24.4 | 25.7 | 25.8 |
| $Fe_2O_3$ | | | | | | | | | | | | | | | | | |
| FeO | 2.7 | 2.4 | 3.5 | 9.0 | 2.0 | 1.9 | 1.8 | 7.6 | 8.1 | 8.4 | 22.3 | 21.8 | 11.8 | 11.4 | 10.3 | 10.6 | 10.6 |
| $Mn_2O_3$ | | | | | | | | | | | | | | | | | |
| MnO | 0.5 | 0.5 | 0.6 | 0.6 | 0.2 | 0.2 | 0.2 | 0.9 | 0.9 | 1.0 | 0.3 | 0.3 | 0.7 | 0.7 | 0.5 | 3.7 | 3.7 |
| MgO | 23.5 | 23.7 | 23.0 | 19.9 | 20.4 | 21.2 | 21.1 | 15.4 | 15.0 | 14.7 | 9.0 | 9.6 | 0.2 | 0.2 | 0.2 | 21.5 | 20.4 |
| CaO | 0.1 | 0.0 | 0.1 | 0.0 | 12.8 | 12.7 | 12.5 | 12.7 | 12.8 | 12.8 | 12.2 | 12.2 | 21.7 | 21.9 | 22.7 | 0.1 | 0.1 |
| $Na_2O$ | 0.4 | 0.4 | 0.3 | 0.3 | 0.4 | 0.6 | 0.5 | 2.7 | 2.7 | 2.7 | 0.3 | 0.3 | 0.0 | 0.0 | 0.0 | 0.1 | 0.0 |
| $K_2O$ | 11.1 | 11.4 | 11.5 | 9.9 | 0.0 | 0.1 | 0.0 | 1.5 | 1.5 | 1.6 | 0.2 | 0.1 | 0.0 | 0.0 | 0.0 | 0.1 | 0.0 |
| Total | 95.7 | 96.1 | 95.6 | 94.6 | 94.8 | 95.2 | 95.1 | 98.3 | 98.9 | 99.2 | 96.8 | 97.8 | 92.9 | 93.4 | 95.5 | 88.0 | 86.2 |
| **Cation ratio** | | | | | | | | | | | | | | | | | |
| O= | 22 | | | | 11 | | | 23 | | | 23 | | 23,OH=3 | | | 28 | |
| Si | 5.45 | 5.45 | 5.37 | 5.42 | 1.25 | 1.29 | 1.31 | 5.91 | 5.84 | 5.82 | 7.69 | 7.75 | 6.12 | 6.12 | 6.02 | 5.18 | 5.15 |
| Ti | 0.00 | 0.01 | 0.01 | 0.02 | 0.00 | 0.00 | 0.00 | 0.01 | 0.02 | 0.02 | 0.00 | 0.00 | 0.03 | 0.04 | 0.01 | 0.00 | 0.00 |
| Al | 3.15 | 3.14 | 3.18 | 3.09 | 3.46 | 3.36 | 3.37 | 2.86 | 2.98 | 2.99 | 0.40 | 0.37 | 4.32 | 4.35 | 4.65 | 5.96 | 6.10 |
| Fe (III) | | | | | | | | | | | | | | | | | |
| Fe (II) | 0.31 | 0.28 | 0.42 | 1.10 | 0.12 | 0.12 | 0.11 | 0.92 | 0.98 | 1.02 | 2.85 | 2.74 | 1.66 | 1.59 | 1.40 | 1.74 | 1.78 |
| Mn(III) | | | | | | | | | | | | | | | | | |
| Mn(II) | 0.06 | 0.06 | 0.07 | 0.07 | 0.01 | 0.01 | 0.01 | 0.11 | 0.11 | 0.12 | 0.04 | 0.03 | 0.10 | 0.10 | 0.07 | 0.62 | 0.63 |
| Mg | 4.94 | 4.96 | 4.89 | 4.35 | 2.17 | 2.24 | 2.22 | 3.34 | 3.23 | 3.18 | 2.06 | 2.16 | 0.06 | 0.06 | 0.04 | 6.30 | 6.12 |
| Ca | 0.01 | 0.01 | 0.01 | 0.00 | 0.98 | 0.96 | 0.94 | 1.98 | 1.99 | 1.99 | 2.01 | 1.96 | 3.90 | 3.92 | 3.94 | 0.01 | 0.01 |
| Na | 0.10 | 0.10 | 0.09 | 0.08 | 0.06 | 0.08 | 0.06 | 0.76 | 0.76 | 0.75 | 0.08 | 0.08 | 0.00 | 0.00 | 0.00 | 0.02 | 0.01 |
| K | 2.00 | 2.05 | 2.09 | 1.84 | 0.00 | 0.01 | 0.00 | 0.28 | 0.28 | 0.30 | 0.03 | 0.03 | 0.00 | 0.00 | 0.00 | 0.02 | 0.00 |
| Total | 16.02 | 16.05 | 16.12 | 15.98 | 8.05 | 8.07 | 8.03 | 16.16 | 16.18 | 16.19 | 15.17 | 15.12 | 16.19 | 16.07 | 16.14 | 19.85 | 19.80 |

TABLE 5. REPRESENTATIVE ELECTRON MICROPROBE ANALYSES OF SPHALERITE ASSOCIATED WITH PYRITE AND/OR PYRRHOTITE.

| | Sphalerite + Pyrrhotite assemblage | | | | | | | | Sphalerite + Pyrite assemblage | | | | | | Sphalerite + Pyrite + Pyrrhotite assemblage | | | | | | |
|---|---|---|---|---|---|---|---|---|---|---|---|---|---|---|---|---|---|---|---|---|---|
| | 1 | 2 | 3 | 4 | 5 | 6 | 7 | 8 | 9 | 10 | 11 | 12 | 13 | 14 | 15 | 16 | 17 | 18 | 19 | 20 | 21 |
| **Weight percent** | | | | | | | | | | | | | | | | | | | | | |
| Cu | 0.0 | 0.0 | 0.1 | 0.1 | 0.1 | 0.0 | 0.0 | 0.0 | 0.0 | 0.1 | 0.1 | 0.0 | 0.0 | 0.0 | 0.1 | 0.0 | 0.1 | 0.1 | 0.0 | 0.1 | 0.0 |
| Fe | 10.0 | 10.4 | 10.8 | 11.0 | 11.1 | 11.5 | 11.9 | 10.8 | 11.1 | 11.5 | 11.6 | 12.6 | 12.9 | 13.3 | 8.4 | 8.7 | 9.0 | 10.2 | 10.3 | 12.0 | 12.6 |
| Zn | 55.5 | 55.1 | 54.8 | 53.4 | 52.8 | 52.0 | 53.7 | 54.1 | 54.2 | 51.9 | 51.6 | 50.2 | 49.4 | 48.6 | 56.9 | 57.0 | 55.8 | 54.0 | 54.2 | 49.0 | 48.3 |
| Mn | 0.7 | 0.8 | 0.8 | 1.8 | 2.0 | 2.4 | 1.0 | 1.0 | 1.4 | 2.8 | 2.6 | 3.3 | 3.8 | 4.3 | 1.2 | 0.9 | 1.4 | 2.1 | 2.2 | 5.0 | 5.3 |
| Cd | 0.1 | 0.1 | 0.1 | 0.1 | 0.1 | 0.1 | 0.1 | 0.1 | 0.0 | 0.1 | 0.1 | 0.1 | 0.1 | 0.1 | 0.1 | 0.1 | 0.1 | 0.1 | 0.0 | 0.1 | 0.1 |
| S | 33.5 | 33.0 | 33.2 | 33.3 | 33.1 | 33.3 | 33.1 | 33.0 | 33.3 | 32.9 | 33.3 | 33.1 | 33.3 | 33.5 | 33.3 | 33.0 | 33.7 | 33.3 | 33.7 | 33.7 | 33.6 |
| Total | 99.8 | 99.4 | 99.6 | 99.5 | 99.2 | 99.3 | 99.7 | 99.0 | 100.1 | 99.2 | 99.1 | 99.3 | 99.4 | 99.8 | 100.1 | 99.7 | 100.1 | 99.7 | 100.4 | 99.8 | 100.0 |
| **Atomic percent** | | | | | | | | | | | | | | | | | | | | | |
| Cu | 0.0 | 0.0 | 0.1 | 0.1 | 0.1 | 0.0 | 0.0 | 0.0 | 0.0 | 0.1 | 0.1 | 0.0 | 0.0 | 0.0 | 0.1 | 0.0 | 0.1 | 0.0 | 0.0 | 0.1 | 0.0 |
| Fe | 8.6 | 8.9 | 9.3 | 9.5 | 9.6 | 9.9 | 10.2 | 9.3 | 9.5 | 9.9 | 10.0 | 10.8 | 11.0 | 11.2 | 7.2 | 7.5 | 7.7 | 8.7 | 8.8 | 10.1 | 10.7 |
| Zn | 40.7 | 40.6 | 40.3 | 39.2 | 38.9 | 38.2 | 39.4 | 40.1 | 39.6 | 38.2 | 37.9 | 36.8 | 36.0 | 35.3 | 41.8 | 42.0 | 40.8 | 39.6 | 39.4 | 35.6 | 35.0 |
| Mn | 0.7 | 0.7 | 0.6 | 1.5 | 1.7 | 2.1 | 0.9 | 0.9 | 1.2 | 2.5 | 2.2 | 2.9 | 3.3 | 3.6 | 1.1 | 0.8 | 1.2 | 1.8 | 1.9 | 4.3 | 4.6 |
| Cd | 0.1 | 0.0 | 0.0 | 0.1 | 0.1 | 0.0 | 0.0 | 0.1 | 0.0 | 0.0 | 0.0 | 0.0 | 0.0 | 0.0 | 0.0 | 0.1 | 0.1 | 0.0 | 0.0 | 0.1 | 0.0 |
| S | 50.1 | 49.6 | 49.7 | 49.8 | 49.7 | 49.8 | 49.5 | 49.7 | 49.6 | 49.4 | 49.9 | 49.5 | 49.6 | 49.8 | 49.9 | 49.6 | 50.2 | 49.8 | 50.0 | 49.9 | 49.7 |
| Mol% FeS | 17.2 | 17.9 | 18.6 | 19.0 | 19.2 | 19.8 | 20.4 | 18.6 | 19.0 | 19.8 | 19.9 | 21.6 | 22.0 | 22.5 | 14.5 | 15.0 | 15.4 | 17.5 | 17.6 | 20.3 | 21.4 |

zone are slightly distinct from those in this study; the La Fortuna garnet in the ore zone is relatively andradite-rich, ranging in $Ad_{26.1-65.7}$. As suggested earlier, however, typical copper skarns show variable compositions of garnet, ranging in approximately $Ad_{30-100}$ (e.g., Einaudi et al., 1981; Meinert, 1992; Meinert et al., 1997). The grossularitic compositions of garnets and the presence of calcic amphiboles (actinolite, pargasitic hornblende) suggest that the exoskarns of the Lambert-Panulcillo belt are relatively aluminous. This would imply that some of the skarns in the Lambert-Panulcillo belt was developed from the surrounding andesite and sandstone.

In contrast to the Panulcillo deposit hosted in the Estratos del Reloj, the other deposits including the La Fortuna occur in the younger Arqueros Formation (Camus, 1986; Ardila, 1993). A strong difference is also present between the Panulcillo and La Fortuna deposit, according to the geochronological data of the related intrusives; the intrusive related to the latter is granodioritic in composition, showing much younger ages (89-98 Ma; Aguirre et al., 1974; 101±5 Ma; A. Sugaki and N. Shimada)[i]. As mentioned earlier, the Panulcillo phlogopite indicates an older mineralization age of ~115 Ma (Ardila, 1993). This age is much younger than that of the dioritic intrusive (~132 Ma) which is clearly related to the primary skarn formation of the Panulcillo deposit. Furthermore, some local zonations of skarn minerals are assumed to have formed by the aplitic dikes at the later stage than the dioritic intrusive (Ardila et al., 1991). Thus, the authors can infer that the above differences in assemblage and composition of skarn minerals would have been induced by both host rocks and intrusives present in the respective areas, and also that the Panulcillo deposit was developed in a complicated process with polymetasomatic reactions.

## SULFIDE MINERALIZATION

Principal sulfide minerals in the ore zone of the Panulcillo deposit appear to have occurred in a nearly simultaneous mineralization with the late stage skarn formation, although two substages are assumed in pyrite formation. Chalcopyrite, the most abundant sulfide, characteristically shows polysynthetic twinning, suggestive of inversion and includes fine-grained star-like crystals of sphalerite. By comparing bulk compositions of the chalcopyrite-sphalerite association in natural ores with the expe-

rimental data on solubility limits of zinc in chalcopyrite (Kojima and Sugaki, 1985); Sugaki et al. (1987) have stated that star-like sphalerite would be formed by unmixing in chalcopyrite. Considering the above two criteria, most star-like crystals of sphalerite are regarded to be a product exsolved from chalcopyrite, which would be the secondary mineral inverted from a precursory Cu-Fe-sulfide.

In contrast, it has been proved that most bleblike and lamellar crystals of chalcopyrite in sphalerite are not due to exsolution (e.g., Sugaki et al., 1987), but replacement (Kojima and Sugaki, 1987) or coprecipitation (Kojima, 1990). Judging from the textural features of the two minerals (Plate 1, Fig. h), the minute inclusions of chalcopyrite in sphalerite are considered to have been epitaxially developed during the growth of host sphalerite.

A pressure-temperature estimate for the sulfide mineralization was not made in the present study, so that the authors cannot quantitatively infer the sulfidation state of the mineralization. The occurrence of monoclinic pyrrhotite may provide a temperature constraint for some of the sulfide mineralization, since this type of pyrrhotite is stable only at temperatures below ~275°C (Sugaki et al., 1977) or ~254°C (Kissin and Scott, 1982). However, it is uncertain whether monoclinic pyrrhotite was stable as a primary mineral. In general, the star-like sphalerite in chalcopyrite is regarded as a relatively high-temperature product, and the measured sphalerite composition (14.4-22.5 mol % FeS) is not consistent with the monoclinic pyrrhotite stable region (ca. 11-18 mol % FeS; Scott and Kissin, 1973). Thus it is highly likely that the sulfide mineralization occurred at higher temperatures than 275-254°C. In such a case, a relatively low-sulfidation assemblage including hexagonal pyrrhotite is assumed to have been stable in the primary ore mineralization. This is compatible with the temperature for the principal stage of mineralization (>320°C) estimated by Ardila et al., 1991). The occurrence of pyrrhotite as a principal mineral is confirmed only at the Panulcillo deposit in the Lambert-Panulcillo belt, although pyrrhotite is reported as a minor mineral in San Antonio district (Ardila et al., 1991). This means that the other deposits in the Lambert-Panulcillo belt were formed under relatively high-sulfidation conditions, and could be a causative factor for the differences in assemblage and composition of the late stage skarn minerals as described earlier.

# CONCLUSIONS

The Panulcillo skarn deposit is regarded to have formed by the reactions of the Valanginian volcano-sedimentary sequence with the Early Cretaceous plutonic rocks, producing high-grade copper ore with chalcopyrite as the principal mineral. Mode of occurrence and chemical compositions of the skarn and ore minerals were examined, and characteristic features were found as follows:

• The exoskarn is composed predominantly of grandite garnet and phlogopite as principal minerals, and pyroxene skarn is observed as a small amount of relict diopside ($Di_{89.6-91.6}$) in the specimens studied.

• Usually the garnet in the ore zone is less andra-ditic ($Ad_{12.9-47.4}$), partially showing anomalous anisotropy under crossed polars.

• The late stage skarn is composed mostly of hydrous minerals such as clintonite, pargasitic hornblende, actinolite, pumpellyite and secondary chlorite.

• Principal ore minerals are chalcopyrite, mono-clinic pyrrhotite, sphalerite, pyrite, and magnetite, generally occurring in the interstices of primary skarn minerals.

• Microscopic features of the ore minerals suggest that most sulfides were formed by a nearly simul-taneous mineralization.

• Chalcopyrite usually exhibits polysynthetic twin-ning, and frequently includes fine skeletal crystals of sphalerite as an exsolution product.

• The sphalerite associated with monoclinic pyr-rhotite and/or pyrite is rich in FeS (14.4 - 22.5 mol%) and MnS (1.6-9.2 mol%) components. The FeS range suggests stability of hexagonal pyrrhotite as the precursory Fe-sulfide phase.

These results reveal that the Panulcillo exoskarn is characterized by Mg-Al-rich compositions, and that the copper mineralization occurred in relatively low-sulfidation environment. The former implies attributions of some dolomitic component in the original carbonate rocks and the surrounding aluminous rocks to the skarn formation. The latter is a characteristic common to world-wide copper skarn deposits associated with barren stocks, but should be considered as an important feature in Cretaceous copper mineralizations of Chile.

# ACKNOWLEDGEMENTS

# REFERENCES

Aguirre, L.; Egert, E. 1965. Cuadrángulo Quebrada Marquesa, Provincia de Coquimbo. *Instituto de Investigaciones Geológicas, Carta Geológica de Chile*, No. 15.

Aguirre, L.; Charrier, L.; Davidson, J.; Mpodozis, C.; Rivano, S.; Thiele, R.; Tidy, E.; Vergara, M.; Vicente, J.C. 1974. Andean magmatism: its paleogeographic and structural setting in the central part of the Southern Andes. *Pacific Geology*, No. 8, p. 1-38.

Ardila, R. 1993. Génesis de los yacimientos de cobre tipo skarn en el distrito minero de San Antonio y el yacimiento Panulcillo, IV Región, Chile. Ph.D. Thesis (Inédito). *Universidad de Chile, Facultad de Ciencias Físicas y Matemáticas*, 234 p.

Ardila, R.; Carrascal, E.R.; Oyarzún, J. 1991. Proposición de un modelo genético para los yacimientos cupríferos tipo skarn de San Antonio y Panulcillo, Región de Coquimbo, Chile. *In Congreso Geológico Chileno, No. 6, Actas*, Vol. 1, p. 256-260. Viña del Mar.

Camus, F. 1986. Los yacimientos estratoligados de Cu, Pb-Zn y Ag de Chile. *In Geología y Recursos Minerales de Chile*, Tomo II (Frutos, J.; Oyarzún, R.; Pincheira, M.; editors). *Universidad de Concepción*, p. 547-635.

Deer, W.A.; Howie, R.A.; Zussman, J. 1962. Rock-forming Minerals, Vol. 3, Sheet silicates. *Longmans*, 270 p. London.

Einaudi, M.T.; Meinert, L.D.; Newberry, R.J. 1981. Skarn deposits. *Economic Geology*, 75th Anniversary Volume, p. 317-391.

González, E. 1954. Estudio geológico-económico del distrito minero de Panulcillo y regiones vecinas. *Anales de la Universidad de Chile, Facultad de Ciencias Físicas y Matemáticas*, Vol. 11, p. 45-93.

Gradstein, F.M.; Ogg, J. 1996. A Phanerozoic time scale. *Episodes*, Vol. 19, Nos. 1-2, p. 3-5.

Hey, M.H. 1954. A new review of the chlorites. *Mineralogical Magazine*, Vol. 30, p. 277-292.

International Mineralogical Association (IMA). 1997. Nomenclature of amphiboles, Report of the subcommittee on amphiboles of the International Mineralogical Association Commission on new minerals and mineral names. *European Journal of Mineralogy*, Vol. 9, p. 623-651.

Ishihara, S.; Ulriksen, C.E. 1980. The magnetite-series and ilmenite-series granitoids in Chile. *Mining Geology*, Vol. 30, p. 183-190.

Ishihara, S.; Ulriksen, C.E.; Sato, K.; Terashima, S.; Sato, T.; Endo, Y. 1984. Plutonic rocks of North-Central Chile. *Geological Survey of Japan, Bulletin*, Vol. 35, p. 503-536.

Kissin, S.A.; Scott, S.D. 1982. Phase relations involving pyrrhotite below 350°C. *Economic Geology*, Vol. 77, p. 1739-1754.

Kitakaze, A. 1996. Cell parameters refinement using Guinier method. *Journal of the Mineralogical Society of Japan*, Vol. 25, p. 69-76 (in Japanese with English abstract).

Kojima, S. 1990. A coprecipitation experiment on intimate association of sphalerite and chalcopyrite and its bearings on the genesis of Kuroko ores. *Mining Geology*, Vol. 40, p. 147-158.

Kojima, S.; Sugaki, A. 1985. Phase relations in the Cu-Fe-Zn-S system between 500° and 300°C under hydrothermal conditions. *Economic Geology*, Vol. 80, p. 158-171.

Kojima, S.; Sugaki, A. 1987. An experimental study on chalcopyritization of sphalerite induced by hydrothermally metasomatic reactions. *Mining Geology*, Vol. 37, p. 373-380.

Leake, B.E. 1978. Nomenclature of amphibole. *American Mineralogist*, Vol. 63, p. 1023-1052.

Mariko, T.; Nagai, Y. 1980. Birefringence and composition of grandite garnet from the Shinyama ore deposit of the Kamaishi mine, Iwate Prefecture, Japan. *Mineralogical Journal*, Vol. 10, p. 181-191.

Meinert, L.D. 1992. Skarn and skarn deposits. *Geoscience Canada*, Vol. 19, p. 145-162.

Meinert, L.D.; Hefton, K.K.; Mayes, D.; Tasiran, I. 1997. Geology, zonation, and fluid evolution of the Big Gossan Cu-Au skarn deposit, Ertsberg district, Irian Jaya. *Economic Geology*, Vol. 92, p. 509-533.

Moscoso, R.; Nasi, C.; Salinas, P. 1982. Hoja Vallenar y parte norte de La Serena, regiones de Atacama y Coquimbo. *Servicio Nacional de Geología y Minería, Carta Geológica de Chile*, No. 55.

Scott, S.D.; Kissin, S.A. 1973. Sphalerite composition in the Zn-Fe-S system below 300°C. *Economic Geology*, Vol. 68, p. 475-479.

Sriramadas, A. 1957. Diagrams for the correlation of unit cell edges and refractive indices with the chemical composition of garnets. *American Mineralogist*, Vol. 42, p. 294-298.

Sugaki, A.; Shima, H.; Kitakaze, A.; Fukuoka, M. 1977. Hydrothermal synthesis of pyrrhotites and their phase relation at low temperature - Studies on the pyrrhotite group minerals (4). *The Science Reports of the Tohoku University*, Series 3, Vol. 8, p. 165-182.

Sugaki, A.; Kitakaze, A.; Kojima, S. 1987. Bulk compositions of intimate intergrowths of chalcopyrite and sphalerite and their genetic implications. *Mineralium Deposita*, Vol. 22, p. 26-32.

Thomas, H. 1967. Geología de la Hoja Ovalle, Provincia de Coquimbo. *Instituto de Investigaciones Geológicas, Boletín*, No. 23, 58 p.

**PLATE 1**

## PLATE 1

Photomicrographs showing mode of occurrences of skarn and ore minerals from the Panulcillo mine

**Figures**

a        Zoned garnet in the skarn zone in plane-polarized light.

b        Identical field to a under crossed polars.

c        Radial clintonite associated with phlogopite under crossed polars.

d        Veinlet of actinolite and chalcopyrite cutting across garnet zone in plane-polarized light.

e        Patchwork-like chalcopyrite filling interstice of garnet grains.

f        Typical association of sulfide minerals in the ore zone.

g        Star-like sphalerite in chalcopyrite.

h        Bleb like and lamellar chalcopyrite parallel with orientation of sphalerite;  **a-d-** transmitted light; **e-h-** reflected light.

**Abbreviations: gt**= garnet; **phl**= phlogopite; **cl**= clintonite; **ac**= actinolite; **py**= pyrite; **po**= pyrrhotite; **cp**= chalcopyrite; **sp**= sphalerite.

PLATE 1